Revisiting LGT Dielectric Constants And Temperature Coefficients Up To 120°C

Peter M. Davulis[1], Blake T. Sturtevant[2], Stephanie L. Duy[1], Mauricio Pereira da Cunha[1]
Dept. of Electrical and Computer Engineering[1], Dept. of Physics[2]
Laboratory for Surface Science and Technology
University of Maine, Orono, Maine USA
mdacunha@eece.maine.edu

Abstract— **Langatate (LGT) has been grown and characterized more intensively in the past decade and the reported acoustic wave properties of this relatively recent crystal have shown significant variations among different groups. Yet to be determined is how much of this dissimilarity is attributable to variations in the growth process or to different measurement techniques. For the dielectric permittivity, in particular, previously published values of $\varepsilon^S_{11}/\varepsilon_0$ differ from each other by as much as 33% while those of $\varepsilon^S_{33}/\varepsilon_0$ differ by up to 25% at room temperature. In this work, the dielectric constants of LGT are determined by measurements made from room temperature (25ºC) up to 120ºC. The permittivity was extracted from capacitance measurements using a precision LCR meter and computer controlled oven. LGT plates oriented along the X, Y, and Z crystalline axes were cut, ground, and polished to an optical finish at the University of Maine's Microwave Acoustic Lab facilities. The capacitor electrodes were deposited using an aerosol spray method chosen for ease of fabrication and to allow for multiple uses of each of the LGT sample. The measured relative dielectric constants reported in this work are: $\varepsilon^S_{11}/\varepsilon_0$ is 17.69 +/- 0.30 and $\varepsilon^S_{33}/\varepsilon_0$ is 70.73 +/- 1.24, which are 11.5% and 7.3% lower then an average of previously published values. The paper discusses the data provided and the associated uncertainties.**

Keywords- LGT, Langatate, Dielectric Permittivity, Temperature Coefficients

I. Introduction

Langatate (LGT, $La_3Ga_{5.5}Ta_{0.5}O_{14}$) belongs to the langasite family of crystals (LGX), which have numerous attractive characteristics, such as higher piezoelectric couple than quartz, the existence temperature compensated orientations, and the absence of phase change up to the melting point, around 1470ºC for LGT [1]. For those reasons, LGX crystals have been considered for a number of acoustic wave applications, including acousto-optic devices; physical, chemical, and biological sensors; filters for wireless and mobile communication; and high temperature applications. LGT, in particular, is a relatively new crystal and the published values of the elastic stiffness, piezoelectricity, dielectric permittivity, and respective temperature coefficients still vary significantly, over 25% for several of these constants among different published works [2]-[11]. In addition, mismatches have been reported between the measured temperature behavior of acoustic wave (AW) devices and the expected responses based on the materials constants and temperature coefficients available [2], [3]. Such inconsistencies compromise prediction regarding propagation properties and, consequently, device modeling and design. For these reasons, the characterization of LGT can benefit from multiple assessments on the measured values of the referred constants and their temperature coefficients, as well as on the measured values of density and the coefficients of thermal expansion.

Regarding the dielectric constants, subject of the present work, two independent dielectric constants need to be measured since LGT is a trigonal class 32 crystal: $\varepsilon_{11}/\varepsilon_0$ and $\varepsilon_{33}/\varepsilon_0$, where ε_0 is the permittivity of free space. The discrepancies in the literature [4]-[11] range from over 33% of their average value for ε_{11} and over 25% of their average value for ε_{33}. For the first order temperature coefficients, TC_1, the published values for ε_{11} and ε_{33} vary in magnitude over 39% and 6%, respectively.

In this paper, the dielectric permittivities of LGT were measured up to 120ºC and compared to published data. The dielectric constants were extracted from capacitance measurements that modeled and accounted for the effects of fringing capacitance. The values of $\varepsilon^S_{11}/\varepsilon_0$ and $\varepsilon^S_{33}/\varepsilon_0$ reported in this work are 11.5% and 7.3%, respectively, lower then an average of previously reported values. Capacitive fringe at the electrode edges was found to account for approximately 9% of the total capacitance. Section II discusses the dielectric constant extraction process and the respective measurement equipment used. In Section III, the measured room temperature dielectric constants and temperature coefficients data are presented, discussed, and compared with the published values. Finally, Section IV concludes the paper.

II. Dielectric Extraction

The dielectric constants were extracted through capacitance measurements of multiple capacitors with different electrode sizes so that the fringe capacitance could be considered. The parallel plate capacitors were made with a ground electrode across one entire face of an LGT plate and the opposite face was partially covered by a circular electrode of a known radius, (Fig. 1). As in [12], the capacitance due to fringing was modeled as proportional to the perimeter of the smaller capacitor electrode. The use of circular electrodes maximizes the area to perimeter ratio. The capacitance of a capacitor with a round electrode is given as:

This project was funded in part by Petroleum Research Fund Grant ACS PRF #42747-AC10, by Army Research Office ARO Grant #DAAD19-03-1-0117, and by National Science Foundation ECS 0134335.

$$C = (\varepsilon_R \, \varepsilon_0 \, \pi \, r^2) \, / \, t + 2\alpha \, \pi \, r, \quad (1)$$

where C = capacitance, ε_R = relative dielectric constant, ε_0 = permittivity of free space, α = fringe capacitance proportionality constant, r = capacitor radius, and t = sample thickness.

Equation (1) can be rewritten in the form of a linear relationship to be

$$(C\,t) \, / \, (\varepsilon_0 \, \pi \, r^2) = (2\alpha/\varepsilon_0)(t\,/r) + \varepsilon_R. \quad (2)$$

Thus making the relative dielectric permittivity the y-axis intercept of the line where the independent variable is t/r and the dependent variable is $(C\,t) \,/\, (\varepsilon_0 \, \pi \, r^2)$, referred to hereafter as the normalized capacitance. As the thickness to radius ratio goes towards zero the normalized capacitance approaches the relative permittivity value.

The extraction process consists of the following: measuring capacitors with different electrode radii; fitting the data to the linear curve given by (2); and finding the relative permittivity from the intercept of that curve with the ordinate axis. The total least squares (TLS) method from [13] was used to fit a straight line to the data because there are uncertainties in both the independent and dependent variables. The best-fit line is obtained by assigning more weight to data points with lower error. The slope and the intercept in (2) with their respective uncertainties were extracted from the fitting.

Capacitance measurements yield the dielectric permittivities measured under constant stress, ε^T_{11} and ε^T_{33}; the dielectric permittivities under constant strain, ε^S_{11} and ε^S_{33}, are calculated by

$$\varepsilon^S_{ij} = \varepsilon^T_{ij} - e_{ip} \, s^E_{pq} \, \underline{e}_{qj} \, , \quad (3)$$

where e_{ip} is the piezoelectric constant tensor, $\underline{e}_{qj}$ is the transposed piezoelectric tensor and s^E_{pq} is the elastic compliance tensor under constant electric field [14]. The LGT elastic and piezoelectric constants used were from [15]. For crystal class 32, ε^T_{33} is equal to ε^S_{33} so only ε^S_{11} needs to be calculated.

The capacitances were measured at eleven temperatures between 25º and 120ºC and the process of finding the dielectric constants was repeated at each temperature. The dielectric constants were fit with a second order polynomial series expansion to extract the temperature coefficients of $\varepsilon^S_{11}/\varepsilon_0$ and $\varepsilon^S_{33}/\varepsilon_0$.

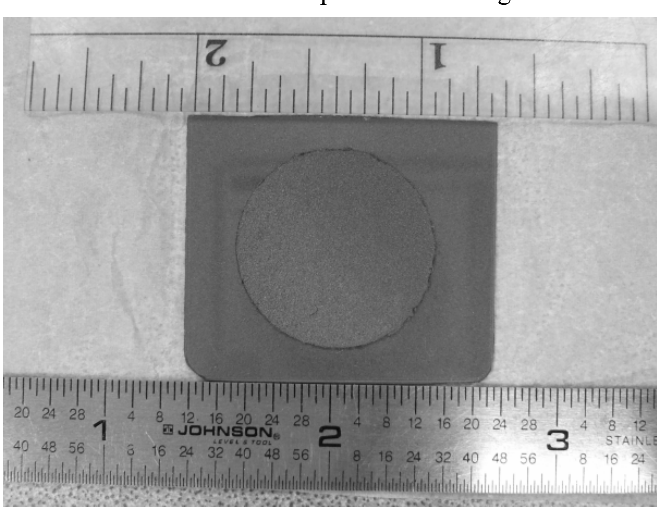

Figure 1. Example capacitor on Y-axis plate, top electrode shown.

The LGT used in this work originated from a boule purchased from Fomos OAS (Moscow, Russia). From the boule, wafers normal to the X, Y, and Z crystalline axes were fabricated at the Microwave Acoustic Materials Laboratory at the University of Maine (UMaine). The wafer orientations were aligned by X-ray diffraction using a PANalytical X'Pert PRO MRD (PANalytical Inc., Natick, MA). An inner diameter saw (Meyer-Berger, Steffisberg, Switzerland) was used to cut the wafers. The wafers were then ground and polished to an optical finish. The wafers thicknesses varied between 0.4 and 0.8 mm and were measured repeatedly using a Heidenhain-Metro precision length gauge (Heidenhain Corp., Schaumburg, IL). The lateral dimensions of the wafers varied between 20 and 40mm. In order to minimize the fringing capacitance with respect to the ideal infinite parallel plate capacitance, the diameters of the capacitors were designed to be at least ten times the thickness of the capacitor wafer.

The wafers were made into capacitors by depositing electrodes on the LGT with conductive nickel aerosol spray (Super Shield, MG Chemicals, Surrey, Canada). The circular capacitors of various sizes were created using masks of low tack dicing tape with punched holes of different sizes. The diameters of the electrodes were measured by photographing the electrode next to rulers. Computer software (GIMP, www.gimp.org) was used to count the number of pixels in an electrode diameter and convert to a physical dimension.

The capacitances of the LGT capacitors were measured at 10kHz with a Precision LCR Meter (Agilent 4284A, Santa Clara, CA). A custom box was fabricated to house and contact the capacitors with pogo-pins, as well as to shield them from electromagnetic interference. The four wires from the LCR meter used in measurement were combined to two wires at the box junction approximately 3cm from the connection to the LGT capacitors. Open and short calibrations were performed before each test. The custom box with the capacitors was kept inside a temperature-controlled oven (Tenney Engineering Inc., Union, NJ). The oven temperature was regulated with a temperature controller (Omega Engineering, Inc., Stamford, CT) and an RTD. The sample temperature was measured with a resolution of 0.1ºC with a separate Omega recorder and an RTD placed inside the capacitor box.

III. RESULTS AND DISCUSSION

The measured room temperature relative dielectric permittivity constants, $\varepsilon^T_{11}/\varepsilon_0$ and $\varepsilon^T_{33}/\varepsilon_0$, along with the calculated $\varepsilon^S_{11}/\varepsilon_0$ are presented in Table 1. The results are listed with a standard deviation which was calculated based on the fitting and the measurement uncertainties. The value of ε^T_{11} was extracted from the best-fit line of the combined X and Y plate data set (Fig. 2). Note that only the error bars in the normalized capacitance are displayed in Fig. 2. This is done for convenience and is justified since the error in the t/r axis is smaller than the error in the normalized capacitance. The largest source of uncertainty in the dielectric extraction is the

TABLE I. LGT DIELECTRIC PERMITTIVITY CONSTANTS AT ROOM TEMPERATURE (25ºC)

Relative Permittivity	This Work	[4]	[5]	[6]	[8]	[9]	[10]	[7,11]
$\varepsilon^T_{11}/\varepsilon_0$	18.57 +/- 0.30 [a]	18.5	20.42 [b]	-	-	19.00 [b]	20.02 [b]	19.9
$\varepsilon^S_{11}/\varepsilon_0$	17.69 +/- 0.30	17.53 [b]	19.6	19.9	26.2	18.271	19.3	19.1
$\varepsilon^S_{33}/\varepsilon_0$	70.73 +/- 1.24	60.9	76.5	78.1	81.9	78.95	80.3	77.2

a. Uncertainty given as standard deviation of variation.

b. Values not reported in respective reference and were calculated from elastic and piezoelectric data in the reference.

patterning of an ideal circular electrode and the measurement of the respective radius, noting that the overall normalized capacitance error varies with the square of the radius. The uncertainty in the normalized capacitance tends to increase as the *t/r* ratio increases, indicating the benefit of having a large radius with respect to the wafer thickness. The conductive spray deposition technique results in a radius error which varies between capacitors due to slightly irregular circular electrodes created.

The capacitance measurements for X and Y plates can be used to independently extract $\varepsilon^T_{11}/\varepsilon_0$, resulting in the values of 18.80 +/- 0.87 and 18.56 +/- 0.54, respectively for the X and Y axes. The permittivities measured along the X and Y axes agree with each other within the uncertainty of the combined final $\varepsilon^T_{11}/\varepsilon_0$. The $\varepsilon^T_{11}/\varepsilon_0$ extracted from the combined data set has a relative uncertainty of 1.6% and the $\varepsilon^T_{11}/\varepsilon_0$ extracted from X and Y data independently had uncertainties of 4.6% and 2.9%, respectively. The combined set has less error because the larger data set results in more confidence in the line fitting and thus in the line intercept.

The $\varepsilon^S_{11}/\varepsilon_0$ found in this work is 11.5% lower than the average of the published values [4]-[11], or 6.7% lower than the average if the reported number in [8], the farthest from the mean, is left out of the average. Only the quantity in [4] is smaller than the one reported in this work. Fig. 3 plots the published values of $\varepsilon^S_{11}/\varepsilon_0$ and the results obtained in this work at room temperature.

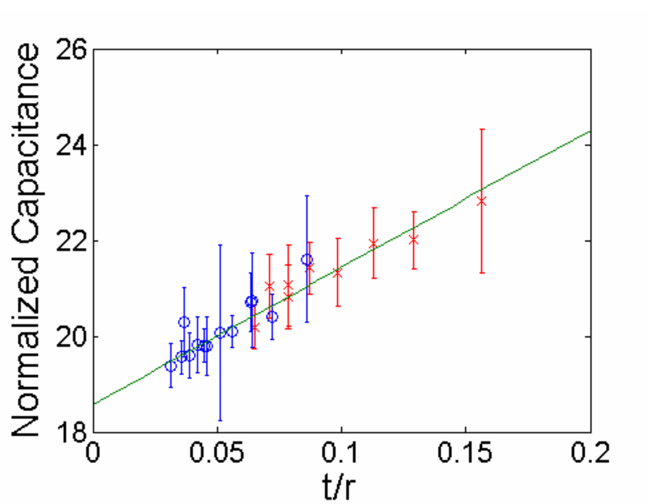

Figure 2. Combined data from X and Y plates. X plate data denoted by x markers with red error bars, Y plate data denoted by o markers with blue error bars, the best fit line is the solid greeen line.

The $\varepsilon^S_{33}/\varepsilon_0$ reported in this work is 7.3% lower the average of published values [4]-[11] or 10.3% lower than the average if the reported number in [4], the farthest from the mean, is left out of the average. Fig. 4 plots the published values of $\varepsilon^S_{33}/\varepsilon_0$ and the results obtained in this work at room temperature.

Figs. 3 and 4 also plot the permittivity constants $\varepsilon^S_{11}/\varepsilon_0$ and $\varepsilon^S_{33}/\varepsilon_0$ as a function of temperature from 25ºC up to 120ºC. Table 2 reports the second order polynomial temperature coefficients of $\varepsilon^S_{11}/\varepsilon_0$ and $\varepsilon^S_{33}/\varepsilon_0$ along with published values [9]-[11]. The first order temperature coefficients determined in this work are of the same order of magnitude as those reported in [9]-[11]. Larger discrepancies are found between the second order coefficients reported in [9] and the remaining published values, including this work. The relative change in the magnitude of $\varepsilon^S_{11}/\varepsilon_0$ from 25˚C to 120˚C is 1.2% while the average relative changes in [9]-[11] is 0.7%. For $\varepsilon^S_{33}/\varepsilon_0$, the relative change in the magnitude is 11.8% and the average of the relative changes in [9]-[11] is 12.8%.

The fringing capacitance was found from dielectric measurements using the slope of the best-fit line from the relative permittivity calculation and compared to the ideal plate capacitance. Utilizing (2) from Section II, the average fringing capacitance was found to have an average value of 9% with respect to the total measured capacitance.

TABLE II. DIELECTRIC PERMITTIVITY TEMPERATURE COEFFICIENTS

	This Work	[9]	[10]	[11]
$\varepsilon^S_{11}/\varepsilon_0$				
TC_1 $[10^{-6}/^oC]$	50.51	-65.480	36.70	38.74
TC_2 $[10^{-9}/^oC^2]$	751.9	-35.960	322.0	539.3
$\varepsilon^S_{33}/\varepsilon_0$				
TC_1 $[10^{-6}/^oC]$	-1512	-1417	-1550	-1593
TC_2 $[10^{-9}/^oC^2]$	3604	-16.1	2300	3187

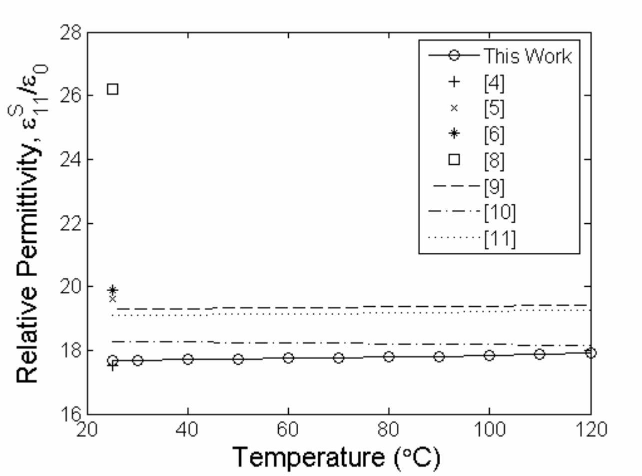

Figure 3. Relative permittivity, $\varepsilon^S_{11}/\varepsilon_0$, plotted with temperature variation of references if available from 25ºC to 120ºC

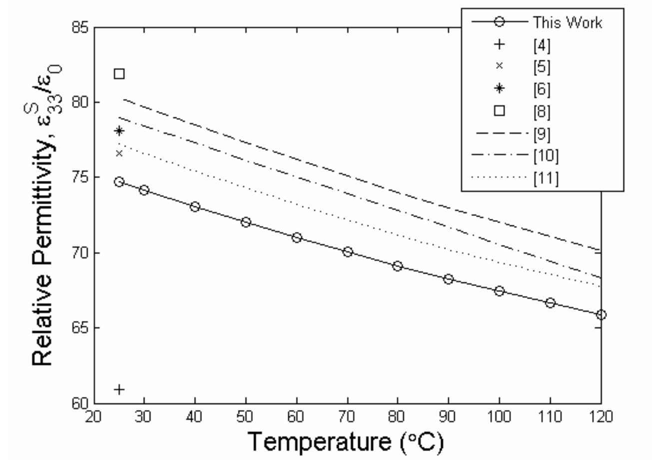

Figure 4. Relative permittivity, $\varepsilon^S_{33}/\varepsilon_0$, plotted with temperature variation if available of references from 25ºC to 120ºC

IV. CONCLUSION

The dielectric permittivities of LGT, $\varepsilon^T_{11}/\varepsilon_0$, $\varepsilon^S_{11}/\varepsilon_0$ and $\varepsilon^S_{33}/\varepsilon_0$ and their temperature coefficients have been determined at temperatures from 25ºC to 120ºC using capacitance measurements and the calculation of the fringing field effects. Both X and Y oriented samples are used to extract $\varepsilon_{11}/\varepsilon_0$ and are consistent within the measurement uncertainty. The dielectric constants $\varepsilon^S_{11}/\varepsilon_0$ and $\varepsilon^S_{33}/\varepsilon_0$ found in this work are 11.5% and 7.3%, respectively, lower than the average of values in the literature. The fringing capacitance was found to account for approximately 9% to the total measured capacitance.

ACKNOWLEDGMENT

The authors wish to thank the personnel of the Laboratory of Surface Science and Technology (LASST) and the Department of Electrical and Computer Engineering.

REFERENCES

[1] J. A. Kosinski, “New piezoelectric substrates for SAW devices,” Int’l J. of High Speed Electronics and Systems, vol. 10, no.4, 2000, pp 1067-1068.

[2] E. Chilla, C. M. Flannery, H.-J. Fröhlich, “Elastic properties of langasite-type crystals determined by bulk and surface acoustic waves,” J. Appl. Phys., vol. 90, no. 12, December 2001, pp 6084-6091.

[3] M. Pereira da Cunha, D. C. Malocha, E. L. Adler, and K. J. Casey, “Surface and pseudo surface acoustic waves in langatate: predictions and measurements,” IEEE Trans. on Ultrason,. Ferroelect., Freq. Contr., vol. 49, no. 9, September 2002, pp 1291-1299.

[4] Y. V. Pisarevsky, P. A. Senyushenkov, B. V. Mill, and N. A. Moiseeva, “Elastic, piezoelectric, dielectric properties of $La_3Ga_{5.5}Ta_{0.5}O_{14}$ single crystals,” Proc. IEEE Int. Freq. Contr. Symp., 1998, pp 742-747.

[5] J. Bohm, E. Chilla, C. Flannery, H.-J. Fröhlich, T. Hauke, R. B. Heimann, M. Hengst, and U. Straube, “Czochralski growth and characterization of piezoelectric single crystals with langasite structure: $La_3Ga_5SiO_{14}$ (LGS), $La_3Ga_{5.5}Nb_{0.5}O_{14}$ (LGN), $La_3Ga_{5.5}Ta_{0.5}O_{14}$ (LGT) II. piezoelectric and elastic properties,” J. Cryst. Growth, vol. 216, 2000, pp. 293–298.

[6] J. Stade, L. Bohaty, M. Hengst, and R. B. Heimaan, “Electro-optic, piezoelectric and dielectric properties of langasite ($La_3Ga_5SiO_{14}$), Langanite ($La_3Ga_{5.5}Nb_{0.5}O_{14}$) and Langataite ($La_3Ga_{5.5}Ta_{0.5}O_{14}$),” Cryst. Res. Technol., vol. 37, no. 10, 2002, pp 1113-1120.

[7] J. Schreuer, “Elastic and piezoelectric properties of $La_3Ga_5SiO_{14}$ and $La_3Ga_{5.5}Ta_{0.5}O_{14}$: an application of resonant ultrasound spectroscopy,” IEEE Trans. on Ultrason,. Ferroelect., Freq. Contr., vol. 49, no. 11, November 2002, pp 1474-1479.

[8] H. Kong, J. Wang, H. Zhang, X. Yin, X. Cheng, Y. Lin, X. Hu, X. Xu, and M. Jiang, “Growth and characterization of $La_3Ga_{5.5}Ta_{0.5}O_{14}$ crystal,” Cryst. Res. Technol., vol. 39, no. 8, 2004, pp 686-691.

[9] D. C. Malocha, M. P. da Cunha, E. Adler, R. C. Smythe, S. Fredrick, M. Chou, R. Helmbold, and Y. S. Zhou, “Recent measurements of material constants versus temperature for lagatate, langanite and langasite,” in Proc. IEEE Freq. Contr. Symp., 2000, pp. 200-205.

[10] N. Onozato, M. Adachi, and T. Karaki, “Surface acoustic wave properties of $La_3Ga_{5.5}Ta_{0.5}O_{14}$ single crystals,” Jpn. J. Appl. Phys., vol. 39, 2000, pp. 3028–3031.

[11] J. Schreuer, J. Rupp, and C. Thybaut, “Temperature dependence of elastic, piezoelectri and dielectric properties of $La_3Ga_5SiO_{14}$ and $La_3Ga_{5.5}Ta_{0.5}O_{14}$: an application of resonant ultrasound spectroscopy,” Proc. IEEE Ultrason. Symp., 2002, pp 373-376.

[12] V. Bottom, “Dielectric constants of quartz,” J. Appl. Phys., vol. 43, no. 4, 1972, pp 1493-1495.

[13] W. H. Press, S. A. Teukolsky, W. T. Vetterling, and B. P. Flannery, Numerical Recipes in C++, Second Edition, New York: Cambridge University Press, 2002, pp 671-675.

[14] IEEE Standard on Piezoelectricity, ANSI/IEEE Std 176-1987, New York, 1988, p 40.

[15] B. T. Sturtevant, P. M. Davulis, and M. Pereira da Cunha, “A new set of LGT constants and temperature coefficients extracted through resonant and pulse echo techniques,” Proc. IEEE Int. Freq. Contr. Symp., 2007, 754-758.